Circular intensity differential scattering of light by hierarchical molecular structures

Chris W. Patterson, Shermila B. Singham, Gary C. Salzman, and Carlos Bustamante

Citation: The Journal of Chemical Physics **84**, 1916 (1986); doi: 10.1063/1.450441
View online: http://dx.doi.org/10.1063/1.450441
View Table of Contents: http://scitation.aip.org/content/aip/journal/jcp/84/3?ver=pdfcov
Published by the AIP Publishing

Circular intensity differential scattering of light by hierarchical molecular structures

Chris W. Patterson, Shermila B. Singham, and Gary C. Salzman
University of California, Los Alamos National Laboratory, Los Alamos, New Mexico 87545

Carlos Bustamante
Department of Chemistry, University of New Mexico, Albuquerque, New Mexico 87131

(Received 12 August 1985; accepted 25 October 1985)

We show that circular intensity differential scattering (CIDS) of light by macromolecules with different levels of chiral structure is the superposition of the CIDS from each individual level. As an example, we treat a model superhelix with anisotropic polarizability.

I. INTRODUCTION

The theory of the circular intensity differential scattering (CIDS) has previously been considered for molecules with one level of chiral structure.[1–8] Biological macromolecules such as chromosomes or plasmids contain complex superstructures built on DNA chains. For such macromolecules CIDS would effectively probe the few levels of structures with dimensions comparable to the wavelength of light being used. The wavelengths chosen for CIDS are in the range 400–500 nm since these are the most easily generated and are not coincident with molecular absorption features of most proteins and nucleic acids.[9] At these wavelengths it is the higher level chiral structures for which CIDS provides information. This is certainly the case for viruses with dimensions of $\approx$200 nm or bacteria with dimensions 1–10 μm. Thus it is important to know the consequences to CIDS when probing the last few levels of chiral structure in a long hierarchical chain.

In this paper we study the CIDS for a model superhelix with two levels of chiral structure. Because we are most often dealing with macromolecules in solution, we will only consider the CIDS resulting from an orientational average. We show that the CIDS of the orientationally averaged superhelix is the superposition of the CIDS for each of the two separate orientationally averaged helices which comprise the superhelix. We give heuristic arguments to show that this superposition principle is quite general and applies to any number and type of chiral structures for which orientational averaging is appropriate. We also give criteria for where the superposition principle is valid.

The consideration of hierarchical structures of molecules also provides an understanding of the theoretical bases for using effective polarizabilities for the "aggregates" which comprise the last level of a macromolecule's structure. It is important to know whether it is possible to average the polarizability of lower order structures in order to obtain effective polarizabilities for higher order structures. In this paper we give examples which help to confirm this averaging principle for anisotropic polarizabilities.

The theory of CIDS for orientationally averaged structures with anisotropic polarizabilities has been developed extensively by Bustamante, Maestre, and Tinoco.[4] We describe this theory briefly below and refer the reader to the referenced work above for more detail.

II. CIDS THEORY FOR SUPERHELIX

We wish to determine the far electric field due to a radiating dipole $\mathbf{p}_i$ at point $\mathbf{r}_i$,

$$\mathbf{p}_i = \hat{\alpha}_i \cdot \mathbf{E}_0, \tag{1}$$

induced by the incident field $\mathbf{E}_0$ where the polarizability at point $\mathbf{r}_i$ is given by

$$\hat{\alpha}_i = \alpha_i \mathbf{e}_i \mathbf{e}_i, \tag{2}$$

where, for convenience, we assume the polarizability is along only one of the three principle axes. The scattered field at $\mathbf{r}'$ with wave vector $\mathbf{k}'$ and incident wave vector $\mathbf{k}$ from a collection of such radiating dipoles is given by

$$E(\mathbf{r}') = Ce^{ik'r'}(\hat{1} - \mathbf{k}'\mathbf{k}') \cdot \sum_i e^{i\Delta\mathbf{k}\cdot\mathbf{r}_i}\hat{\alpha}_i \cdot \mathbf{E}_0, \tag{3}$$

where

$$\Delta\mathbf{k} = \mathbf{k}' - \mathbf{k}'. \tag{4}$$

The orientational average for the intensity difference $I_L - I_R$ between left and right circularly polarized light given by Bustamante *et al.*[4] is then

$$\begin{aligned} I_L - I_R = {} & (C/2)\sum_{i,j}\alpha_i^*\alpha_j(\mathbf{e}_i \times \mathbf{e}_j) \\ & \cdot \hat{R}_{ij}\{[(\mathbf{e}_i \cdot \mathbf{e}_j)(j_2/q - j_1) \\ & - (\mathbf{e}_i \cdot \hat{R}_{ij})(\mathbf{e}_j \cdot \hat{R}_{ij})(5j_2/q - j_1)](\sin\beta + \sin^3\beta)\}, \end{aligned} \tag{5}$$

where the arguments of the spherical Bessel functions

$$q = 4\pi R_{ij}/\lambda \tag{6}$$

are omitted for simplicity and

$$\mathbf{R}_{ij} = \mathbf{r}_j - \mathbf{r}_i \tag{7}$$

is the distance vector between dipoles. The angle β is half the scattering angle and is 90° for backward scattering.

Equation (5) is the starting point for all our calculations of CIDS arising from helices and superhelices. Although normally the CIDS signal is normalized to the total scattered intensity $I_L + I_R$, we shall see that such a normalization conceals the superposition principle which we develop below. As a result, we shall identify CIDS as synonymous with the orientationally averaged $I_L - I_R$ given in Eq. (5). When calculating CIDS using Eq. (5) we let $C = 1$ and $\alpha = 1$.

For the examples of the superposition principle given below we will be concerned with helical supercoiling. The CIDS due to simple helices has already been studied extensively by Bustamante *et al.* and we shall rely heavily upon

 0021-9606/86/031916-06$02.10

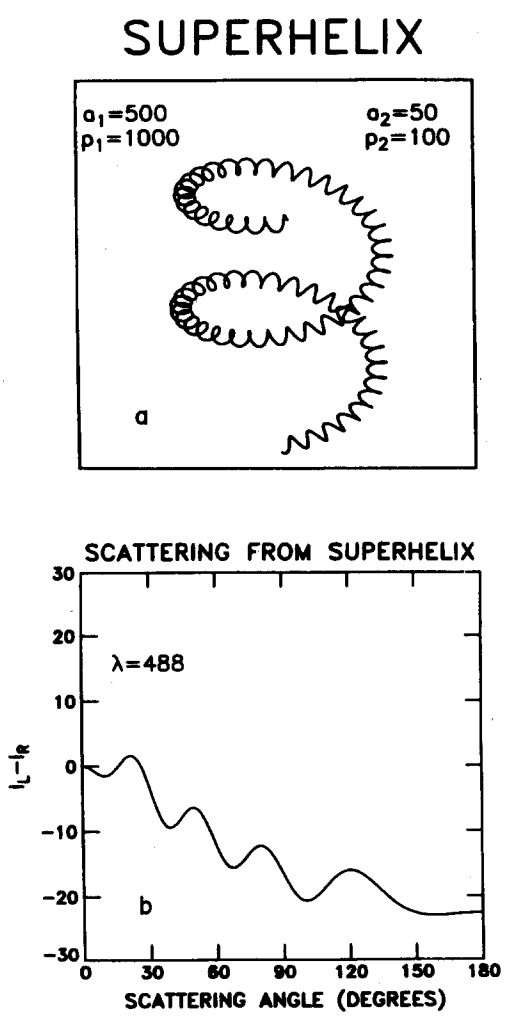

FIG. 1. (a) Superhelix with radius and pitch dimensions shown. (b) CIDS from one turn of superhelix with three dipoles per turn of small helix. The dipoles are directed tangential to the superhelix. A total of 96 dipoles were used.

their results. In parametric form the position vector for a right handed helix with radius a_1 and pitch p_1 is given by

$$\mathbf{r} = (a_1 \cos\theta)\mathbf{i} + (a_1 \sin\theta)\mathbf{j} + (p_1\theta/2\pi)\mathbf{k}. \tag{8}$$

We may define mutually orthogonal unit vectors which are normal, tangential, and perpendicular to the helix at every point:

$$\mathbf{n} = \cos\theta\mathbf{i} + \sin\theta\mathbf{j},$$

$$\mathbf{t} = \frac{1}{M}\frac{d\mathbf{r}}{d\theta} = -(a_1/M)\sin\theta\mathbf{i} + (a_1/M)\cos\theta\mathbf{j} + (p_1/2\pi M)\mathbf{k},$$

$$\mathbf{p} = \mathbf{t}\times\mathbf{n} = -(p_1/2\pi M)\sin\theta\mathbf{i} + (p_1/2\pi M)\cos\theta\mathbf{j} - (a_1/M)\mathbf{k}, \tag{9}$$

where the normalization constant M is given by

$$M = (a_1^2 + p_1^2/4\pi^2)^{1/2}.$$

By analogy, the position vector for a superhelix with primary radius a_1 and pitch p_1 and secondary radius a_2 and pitch p_2 is

$$\mathbf{r}' = \mathbf{r} + a_2\cos\varphi\mathbf{n} + a_2\sin\varphi\mathbf{p}, \tag{10}$$

where

$$\varphi = M\theta/p_1.$$

We may then define three mutually orthogonal unit vectors at any point on the superhelix:

$$\mathbf{n}' = \cos\varphi\mathbf{n} + \sin\varphi\mathbf{p},$$

$$\mathbf{t}' = \frac{1}{M'}\frac{d\mathbf{r}'}{d\varphi},$$

$$\mathbf{p}' = \mathbf{t}'\times\mathbf{n}', \tag{11}$$

where M' is the normalization constant for $\mathbf{t}'$. The polarizability tensor $\hat{\alpha}_i$ at any point on the superhelix may then be written in terms of these unit vectors as in Eq. (2).

III. SUPERPOSITION PRINCIPLE

We now apply Eq. (5) to calculate the CIDS from the superhelix shown in Fig. 1(a). The result is shown in Fig. 1(b) where we have assumed the polarization is in the tangential direction ($\mathbf{e}_i = \mathbf{t}'$). One can observe in Fig. 1(b) a high frequency oscillation superimposed on a low frequency one. In general, the higher frequency oscillation in reciprocal **k** space of CIDS corresponds to the larger structure in real **r** space. One might expect, then, that the observed high and low frequency oscillations in Fig. 1(b) might corre-

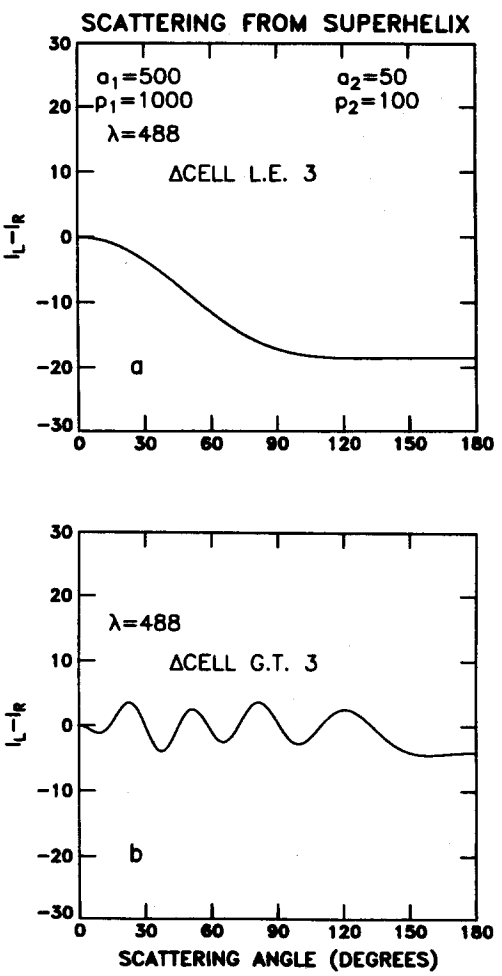

FIG. 2. CIDS from superhelix shown in Fig. 1 with (a) interference terms between dipoles differing by three turns of the small helix or less and (b) interference terms between dipoles differing by more than three turns of the small helix. The sum of CIDS in (a) and (b) here is by definition exactly the CIDS shown in Fig. 1(b).

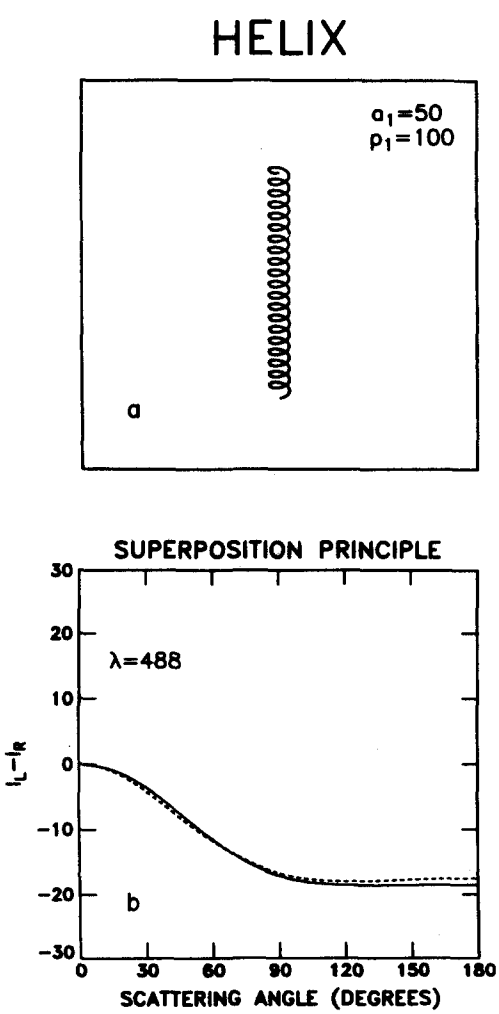

FIG. 3. (a) Small helix of the superhelix with radius and pitch dimensions shown. (b) CIDS from the small helix (dashed line) is compared with the CIDS in Fig. 2(a) (solid ine). We use 32 turns of the small helix with three dipoles per turn. The dipoles are directed tangential to the helix.

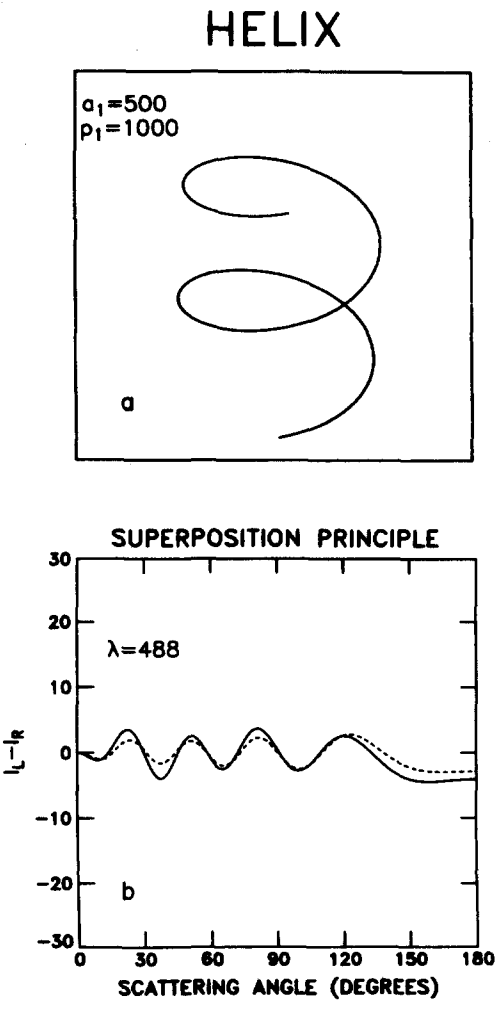

FIG. 4. (a) Large helix of the superhelix with radius and pitch dimensions shown. (b) CIDS from the large helix (dashed line) is compared with the CIDS in Fig. 2(b) (solid line). We use one turn of the large helix with 96 evenly spaced dipoles corresponding to those translated from the superhelix in Fig. 1.

spond to the CIDS of the large and small helices, respectively, in Fig. 1(a).

In order to see this behavior, we partition the sum in Eq. (5) into two separate sums—one where dipoles i and j differ by less than (or equal to) three "cells" (turns of the small helix) and the other where dipoles i and j differ by greater than three cells. That is, if ic designates the cell number and ip the dipole number within the cell, we may write the sum in Eq. (5) as simply

$$\sum_{i,j} \equiv \sum_{ip,jp\in\{|ic-jc|<3\}} + \sum_{ip,jp\in\{|ic-jc|>3\}}, \tag{12}$$

where each cell has the same number of dipoles. For the superhelix we are considering, the first sum in the above partition is shown in Fig. 2(a) while the second sum in the above partition is shown in Fig. 2(b). By the above procedure we have succeeded in partitioning the CIDS in Fig. 1 into a component with a low frequency oscillation and another with a high frequency oscillation. We find that the partitioned CIDS is rather insensitive to our choice of cutoff $|ic-jc|=3$.

For the superhelix shown in Fig. 1 there are $M/p_2 \cong 33$ cells of the small helix per turn of the large helix. Our choice of the cutoff was made such that the first sum in the partition in Eq. (12) included mainly interference effects from the small helix while the second sum included mainly interference effects from the large helix. Thus one would expect the CIDS in Fig. 2(a) to be due mainly to the small helix and the CIDS in Fig. 2(b) to be due mainly to the large helix.

Furthermore, *the CIDS $I_L - I_R$ from a given helix is insensitive to its length*! This result is in contrast to that for the normalized CIDS $(I_L - I_R)/(I_L + I_R)$ which can be sensitive to length when the pitch or radius of the helix exceeds the wavelength λ. Thus the CIDS in Figs. 2(a) and 2(b) arising from the small and large helices, respectively, are insensitive to the cutoff chosen for the partitioning in Eq. (12). Indeed, we obtain similar results for a cutoff between 2 and 5.

The partitioning of the CIDS signal into hierarchical components by using Eq. (12) is the essence of the superposition principle. It is important that the hierarchical structures have disparate scales for the partitioning to be successful. Furthermore, it is necessary that each level have a chiral structure that can result in a CIDS. These two criteria are certainly obeyed by the superhelix shown in Fig. 1. It remains to be shown that the CIDS in Figs. 2(a) and 2(b) do indeed correspond to the CIDS of the small and large helical

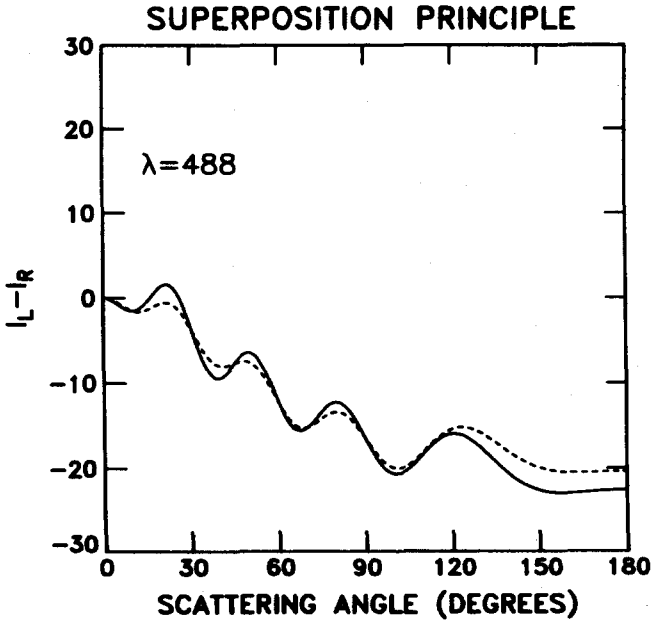

FIG. 5. Comparison of the CIDS from the superhelix in Fig. 1 (solid line) with the sum of the CIDS from the individual small and large helices (dashed line). The dashed line here is the sum of the dashed lines in Figs. 3(b) and 4(b).

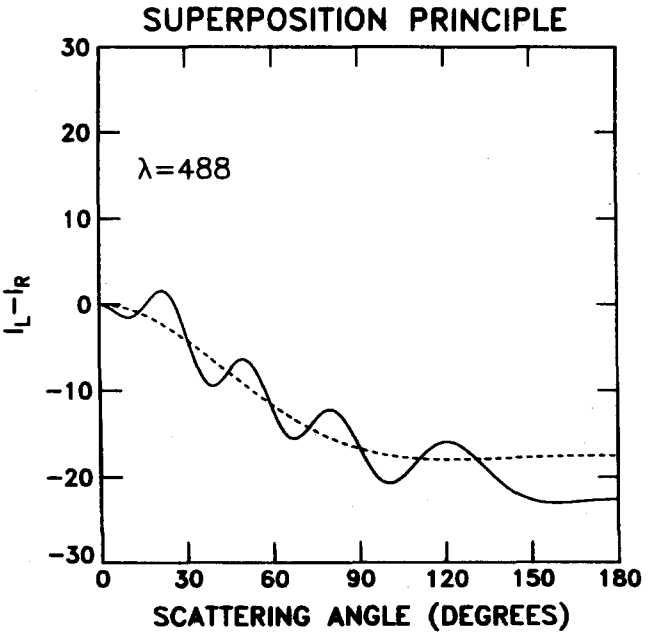

FIG. 6. Comparison of the CIDS from the superhelix in Fig. 1 (solid line) with the CIDS from the small helix (dashed line).

components of the superhelix.

In Fig. 3 the CIDS from the small helix with tangential polarizability is compared with the partitioned CIDS in Fig. 2(a), while in Fig. 4 the CIDS from the large helix is compared with the partitioned CIDS in Fig. 2(b). In Fig. 5 we compare the superposition of the CIDS from the large and small helix with the unpartitioned CIDS from the superhelix. The agreement is quite good and confirms the superposition principle. Note that, in general, the superposition principle would not work had we followed standard procedure and normalized the CIDS with the total intensity $I_L + I_R$.

An important question arises as to what polarizability one uses for the large helix. We place the dipoles on the large helix by assuming that $a_2 = 0$ for the superhelix. Consistent with this assumption, we simply translate the dipole vectors of the superhelix to their new position on the large helix. Calculations show that such a translation is possible when

$$a_2 \ll a_1, p_1. \tag{13}$$

Calculations have also shown that further simplification is possible. We may average the dipole vector over the turns of the small helix when

$$p_2 \ll a_1, p_1. \tag{14}$$

Such an average results in only a tangential component of the induced dipole on the large helix:

$$\langle \mathbf{n}' \rangle \cong 0, \tag{15a}$$

$$\langle \mathbf{t}' \rangle \cong (p_2/2\pi M')\mathbf{t}, \tag{15b}$$

$$\langle \mathbf{p}' \rangle \cong (a_2/M')\mathbf{t}, \tag{15c}$$

where

$$M' \cong (a_2^2 + p_2^2/4\pi^2)^{1/2}.$$

That is, as a consequence of the averaging, we may project the dipole vectors of the small helix onto the large helix to obtain an effective polarization for the large helix. We have indeed used the approximation Eq. (15b) in Fig. 4 to find the CIDS for the large helix. The amplitude of the CIDS in Fig. 4 is relatively small since $(p_2/2\pi M') = 0.303$ and the polarizability is squared in the expression for CIDS.

In actual practice one has a CIDS signal and is faced with the task of separating the small and large oscillation so that the CIDS can be analyzed separately for each structural level. In Fig. 6 we compare the CIDS from the small helix with the CIDS for the superhelix. It is evident that the CIDS of the superhelix oscillates about the CIDS of the small helix. This is just a representation in reciprocal space of the fact that the superhelix oscillates about the large helix in real space! Thus the difference of scales of hierarchical levels in real space implies different scales of hierarchical levels in CIDS as well. If one can see the hierarchy in real space due to the disparate scales, then one can see it in the CIDS as well.

The existence of a discernible hierarchy in CIDS allows one to apply a smoothing function or high frequency filter to extract the CIDS arising from the small structure component. For multiple levels of molecular structure, such a smoothing function can be applied repetitively and the CIDS signal at each level, starting with the largest molecular structure, can be extracted sequentially until only the CIDS from the smallest component of molecular structure remains. Conversely, if there is no visually discernible hierarchy in real space, there will be none in the CIDS. Signal smoothing will not work and the superposition principle will not apply.

As a more stringent test of the superposition principle, we find the CIDS from the superhelix shown in Fig. 7 where there are $M/p_2 \cong 13$ turns of the small helix per turn of the large helix. Again we use tangential polarizability ($\mathbf{e}_i = \mathbf{t}'$).

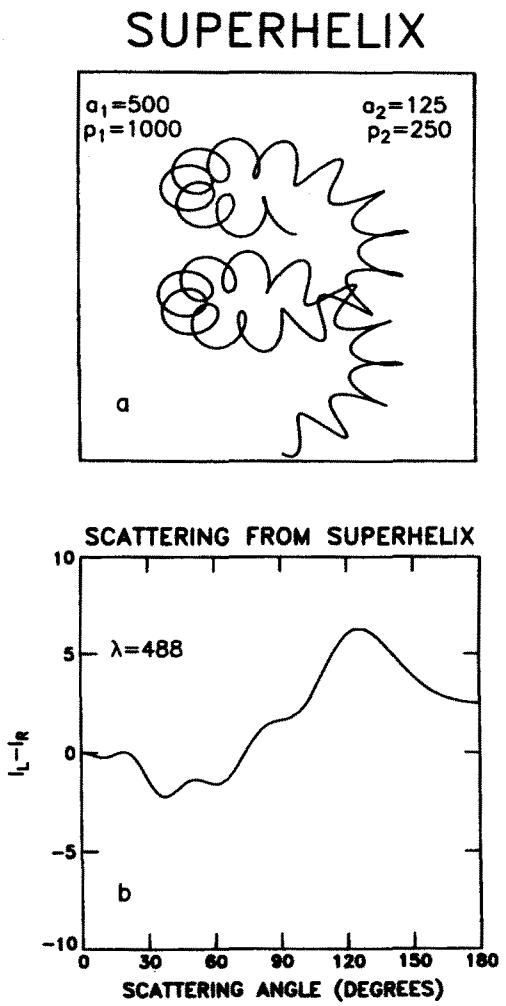

FIG. 7. (a) Superhelix with radius and pitch dimensions shown. (b) CIDS from one turn of superhelix with three dipoles per turn of the small helix. The dipoles are directed tangential to the superhelix. A total of 39 dipoles were used.

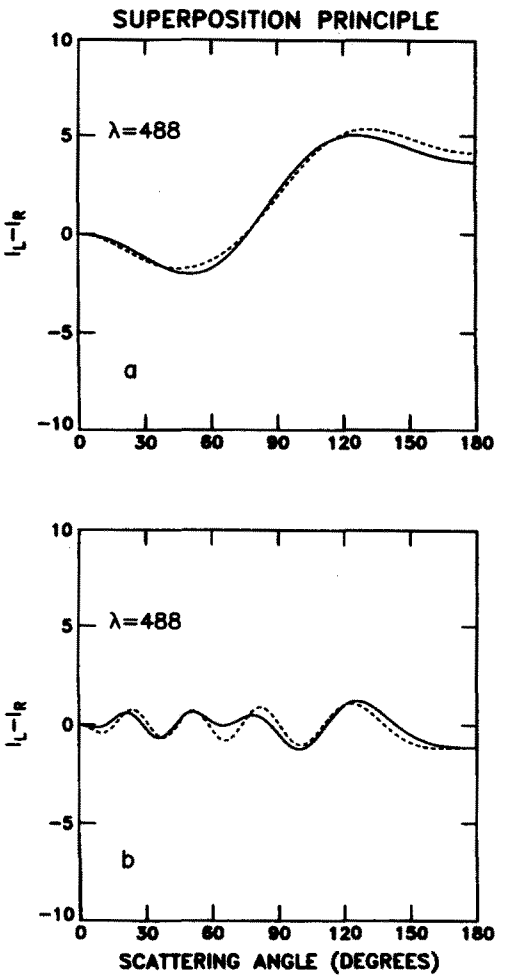

FIG. 8. (a) CIDS from the small helix with $a_2 = 125$ and $p_2 = 250$ (dashed line) is compared with the partitioned CIDS (see the text) from the superhelix in Fig. 7 (solid line). For the small helix we used 13 turns with three dipoles per turn. (b) CIDS from the large helix with $a_1 = 500$ and $p_1 = 1000$ (dashed line) is compared with the partitioned CIDS (see the text) from the superhelix in Fig. 7 (solid line). For the large helix we used one turn with 39 evenly spaced dipoles.

The decomposition of the CIDS into components with low and high frequency oscillations is now more sensitive to the cutoff point which we take to be two cells. In Figs. 8(a) and 8(b) we compare the CIDS from the small and large helix with the partitioned CIDS of the superhelix. Finally, in Fig. 9 we compare the superimposed CIDS of the small and large helix with the CIDS from the superhelix. The agreement is surprising in view of the fact that conditions given by Eqs. (13) and (14) are not obeyed. Although we used tangential polarizability ($\mathbf{e}_i = \mathbf{t}$) for the large helix, we adjusted α to obtain agreement at 180° in Fig. 8(b) since Eq. (15b) was no longer valid.

The fact that tangential polarizability can be used for the large helix independent of the polarizability chosen for the superhelix itself ($\mathbf{e}_i = \mathbf{n}'$, $\mathbf{p}'$, or $\mathbf{t}'$) is an important result. This result confirms the hypothesis of Bustamente *et al.*[4] that one can use tangential polarizability when the highest structural level is an helix. Indeed, all the modeling by Bustamante *et al.* was for such a polarizability and there was agreement with the CIDS experiment on helical octopus sperm.[10] It is reasonable to assume this agreement was the result of the effects of the polarizability being averaged over lower order structure as in our examples.

IV. CONCLUSIONS

We have shown that the CIDS arising from chiral molecules with hierarchical levels of structure is the superposition of CIDS from each of the individual levels. For the superposition principle to be valid, it is necessary that the CIDS result from an orientational average of the macromolecule and that the different levels of structure be readily discernible. Furthermore it is necessary that the CIDS for each level be independent of the structural length. The later is a unique property of CIDS that makes the superposition principle of general validity independent of the particular chiral structure.

The basis for the superposition principle stems from the ability to partition the intensity sum in Eq. (12) into partial sums which separate the CIDS into hierarchical levels of structure in reciprocal space. The validity of this partition is difficult to prove rigorously and we have only given intuitive arguments in this paper. Indeed, if the conditions in Eqs.

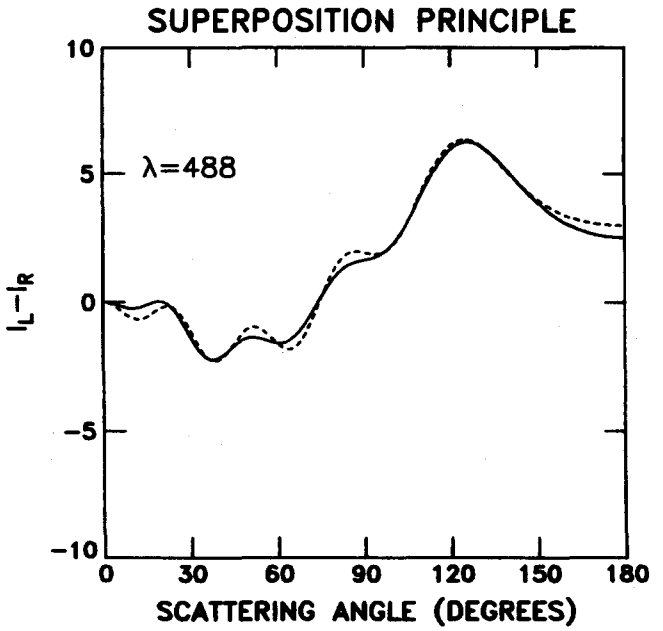

FIG. 9. Comparison of the CIDS from the superhelix of Fig. 7 (solid line) with the sum of the CIDS from the individual small and large helices (dashed line). The dashed line here is the sum of the dashed lines in Figs. 8(a) and 8(b).

(13) and (14) are obeyed, then the interference terms between the small and large helices of the superhelix are small and the superposition principle is valid. However, even when these conditions are not met one can get cancellation of the relatively large interference terms between the helices such that the superposition principle is still valid. Thus it is difficult to prove the full range of validity of this principle. Although we have only applied the superposition principle to two levels of structure, using the superhelix as an example, it may readily be extended to more levels of structure and to different chiral geometries.

The superposition principle allows us to treat the different levels of structure of a macromolecule on an equal footing. This is a result which differs from the more familiar examples in x-ray crystal diffraction. Indeed, the primitive unit cell for the superhelix, which may be repeated by simple translation, is the turn of the large helix (assuming it contains an integral number of turns of the small helix). In crystallography it is this cell which is responsible for the overall diffraction pattern in reciprocal space. The substructure due to the small helix would result in a geometrical structure *factor* modifying the intensities of this diffraction pattern. In the case of CIDS, the small helix moderates the pattern due to the large helix by *superposition* instead of *factorization*. Thus the process of convolution in real space corresponds to a sum in reciprocal space for CIDS instead of a factor in reciprocal space as for the case of crystal diffraction.

Finally, we should mention that $I_L - I_R$ is equivalent to the S_{14} component of the Muller matrix which describes the general scattering of light by the medium.[11] Crystal diffraction of light is concerned with the element S_{11} describing the total scattering intensity. Preliminary calculations indicate that the superposition principle is valid for the components S_{24} and S_{34} as well as for S_{14} under similar conditions. We have also obtained encouraging results for isotropic polarizabilities. We hope to investigate this behavior in a future work.

ACKNOWLEDGMENTS

This work was carried out under the auspices of the U. S. Department of Energy and was supported in part by Mesa Diagnostics, Inc., Los Alamos, NM.

[1]C. Bustamante, M. F. Maestre, and I. Tinoco, Jr., J. Chem. Phys. **73**, 4273 (1980).
[2]C. Bustamante, M. F. Maestre, and I. Tinoco, Jr., J. Chem. Phys. **73**, 6046 (1980).
[3]C. Bustamante, I. Tinoco, Jr., and M. F. Maestre, J. Chem. Phys. **74**, 4839 (1981).
[4]C. Bustamante, I. Tinoco, Jr., and M. F. Maestre, J. Chem. Phys. **76**, 3440 (1982).
[5]S. Zietz, A. Belmont, and C. Nicolini, Cell Biophys. **5**, 163 (1983).
[6]W. M. McClain, J. A. Schauerte, and R. A. Harris, J. Chem. Phys. **80**, 606 (1984).
[7]C. Bustamante, M. Maestre, D. Keller, and I. Tinoco, Jr., J. Chem. Phys. **80**, 4817 (1984).
[8]D. Keller, C. Bustamante, M. Maestre, and I. Tinoco, Jr., Biopolymers **24**, 783 (1985).
[9]G. Salzman and C. Gregg, Biotechnology, March 1984.
[10]M. F. Maestre, C. Bustamante, T. L. Hayes, J. A. Subirana, and I. Tinoco, Jr., Nature **298**, 773 (1982); I. Tinoco, Jr. and A. L. Williams, Jr., Annu. Rev. Phys. Chem. **35**, 329 (1984).
[11]C. F. Bohren and D. R. Huffman, *Absorption and Scattering of Light by Small Particles* (Wiley, New York, 1983), p. 63.